



ELSEVIER



CrossMark

BASIC SCIENCE

Nanomedicine: Nanotechnology, Biology, and Medicine  
13 (2017) 933–942



nanomedjournal.com

Original Article

# Assessment of *in vivo* systemic toxicity and biodistribution of iron-doped silica nanoshells

Natalie Mendez, MS<sup>a</sup>, Alexander Liberman, PhD<sup>a</sup>, Jacqueline Corbeil, BS<sup>b</sup>,  
Christopher Barback, BS<sup>b</sup>, Robert Viveros, BS<sup>a</sup>, James Wang, MS<sup>a</sup>,  
Jessica Wang-Rodriguez, MD<sup>c</sup>, Sarah L. Blair, MD<sup>d</sup>, Robert Mattrey, MD<sup>b</sup>, David Vera, MD<sup>b</sup>,  
William Trogler, PhD<sup>e</sup>, Andrew C. Kummel, PhD<sup>e,\*</sup>

<sup>a</sup>Department of Materials Science and Engineering, Nanoengineering, and Chemical Engineering, University of California, San Diego, CA, USA

<sup>b</sup>Department of Radiology, University of California, San Diego, CA, USA

<sup>c</sup>Department of Pathology, University of California, San Diego, CA, USA

<sup>d</sup>Department of Surgery, University of California, San Diego, CA, USA

<sup>e</sup>Department of Chemistry and Biochemistry, University of California, San Diego, CA, USA

Received 5 May 2016; accepted 18 October 2016

## Abstract

Silica nanoparticles are an emerging class of biomaterials which may be used as diagnostic and therapeutic tools for biomedical applications. In particular, hollow silica nanoshells are attractive due to their hollow core. Approximately 70% of a 500 nm nanoshell is hollow, therefore more particles can be administered on a mg/kg basis compared to solid nanoparticles. Additionally, their nanoporous shell permits influx/efflux of gases and small molecules. Since the size, shape, and composition of a nanoparticle can dramatically alter its toxicity and biodistribution, the toxicology of these nanomaterials was assessed. A single dose toxicity study was performed *in vivo* to assess the toxicity of 500 nm iron-doped silica nanoshells at clinically relevant doses of 10–20 mg/kg. This study showed that only a trace amount of silica was detected in the body 10 weeks post-administration. The hematology, biochemistry and pathological results show that the nanoshells exhibit no acute or chronic toxicity in mice.

© 2016 Elsevier Inc. All rights reserved.

**Key words:** Silica nanoparticles; Toxicity; Biodistribution; Biomaterials; Toxicology; Nanomaterials

Silica (SiO<sub>2</sub>) nanomaterials have gained much attention due to their broad range of potential biomedical applications which include bio-imaging, drug delivery, biosensors, and therapeutic

ablation.<sup>1–3</sup> Characteristics that make SiO<sub>2</sub> nanoparticles a promising material are their well-established surface modification chemistry, high surface area, large pore volume, high

**Abbreviations:** ICP-OES, inductively coupled plasma optical emission spectroscopy; IV, intravenous; mesoporous silica nanoparticle, MSN; Tetramethyl orthosilicate, TMOS; energy dispersive X-ray spectroscopy, EDX; complete blood count, CBC; hematoxylin and eosin, H&E; scanning electron microscopy, SEM; high intensity focused ultrasound, HIFU; alanine transaminase, ALT; alkaline phosphatase, ALP; blood urea nitrogen, BUN; phosphate buffered saline, PBS; SiO<sub>2</sub>, silica; Fe-SiO<sub>2</sub>, iron-silica.

This research was supported by National Institutes of Health IMAT 1R33CA177449-01A1 and the National Institutes of Health Cross Training Translation Cancer Researchers in Nanotechnology (CRIN) Support (National Institutes of Health Grant No. 3 R25 CA 153915-03S1). Individual student funding was provided by the NCI Research Supplements to Promote Diversity in Health Related Research Fellowship (National Institutes of Health Grant No. 1R33CA177449-01A1). The authors thank Dr. K. Pestonjamas and the rest of the Cancer Center Microscopy Core Facility at UCSD (NCI Grant No. P30 CA23100) and the UCSD Histology and Immunohistochemistry core facility.

A.C. Kummel and W.C. Trogler have an equity interest in Nanocyte Medical, Inc., a company that may potentially benefit from the research results, and also serve on the company's Scientific Advisory Board. S.L. Blair has a family member with an equity interest in Nanocyte Medical, Inc., a company that may potentially benefit from the research results. The terms of this arrangement have been reviewed and approved by the University of California, San Diego in accordance with its conflict of interest policies.

\*Corresponding author at: University of California, San Diego, Chemistry & Biochemistry, La Jolla, CA 92093-0358.

E-mail address: akummel@ucsd.edu (A.C. Kummel).

<http://dx.doi.org/10.1016/j.nano.2016.10.018>

1549-9634/© 2016 Elsevier Inc. All rights reserved.

stability in storage, and *in vivo* stability.<sup>4,5</sup> Furthermore, porous SiO<sub>2</sub> nanoshells have gained considerable interest as *in vivo* imaging agents due to their potential to improve cancer diagnosis and their ability to provide guidance during surgery.<sup>6–8</sup> SiO<sub>2</sub> nanoshells can be used as carriers for contrast agents such as a fluorophore,<sup>9,10</sup> perfluorocarbon,<sup>8,11</sup> and superparamagnetic material.<sup>12–14</sup>

Many studies have evaluated the toxicity of various SiO<sub>2</sub> nanoparticle formulations. The size, shape, morphology, charge, and surface properties of a nanoparticle can dramatically affect its biodistribution and toxicology.<sup>3</sup> For instance, solid SiO<sub>2</sub> materials with amorphous particle morphology may cause hemolysis of red blood cells, which raises concerns regarding their safety in the clinic.<sup>15,16</sup> Yu et al (2011) investigated the impact of SiO<sub>2</sub> nanoparticle design on cellular toxicity and hemolytic activity up to 500 µg/ml by evaluating the effect of geometry, size, porosity, and surface charge of SiO<sub>2</sub> nanoparticles *in vitro*.<sup>17</sup> It was shown that the toxicity of SiO<sub>2</sub> nanoparticles is influenced by surface charge and pore size and that cellular toxicity is cell-type dependent. Their studies showed that solid nonporous nanoparticles had a far greater hemolytic activity compared to mesoporous silica nanoparticles (MSNs), which showed no hemolytic toxicity for all geometries, at doses below 100 µg/mL.

Several *in-vivo* studies have been performed to assess the toxicity of SiO<sub>2</sub> nanoparticles. They show that SiO<sub>2</sub> nanoparticles can cause inflammatory responses and hepatotoxicity which are influenced by factors such as dose, particle size, surface area, charge, and particle formulation.<sup>9,17–21</sup> For example, Yu et al investigated the acute toxicity of 120 nm spherical MSNs when administered intravenously (IV)<sup>22</sup>; the maximum tolerated dose for these particles was 30 mg/kg. Nishimori et al investigated the relationship between particle size and toxicity using nonporous spherical SiO<sub>2</sub> particles with diameters of 70 nm, 300 nm and 1000 nm.<sup>23</sup> Their findings showed that 70 nm nanoparticles induced liver injury at 30 mg/kg, while 300 nm and 1000 nm SiO<sub>2</sub> particles exhibited no biochemical or histological tissue damage even at 100 mg/kg. This shows that the size of the nanoparticle can significantly alter the toxicity even for the same particle formulation.

The biodistribution of nanoparticles provides some information of the excretion and degradability of the administered particles. Several studies have examined the biodistribution of SiO<sub>2</sub> particles, which have shown them to primarily accumulate in mononuclear phagocyte system (MPS) organs such as the liver, lungs and spleen. Studies have shown that SiO<sub>2</sub> nanoparticles can be excreted from the body; the excretion is influenced by particle formulation, size, dose, and surface modification, among other factors.<sup>4,11,24,25</sup> It is expected that these factors will also influence the toxicity.

Before new nanomaterial formulations can be applied safely in a clinical setting, their biocompatibility and biodistribution need to be assessed. Despite the numerous studies of the toxicology of various forms of SiO<sub>2</sub> nanoparticles, the toxicity of each formulation must be assessed before being translated to the clinic, since nanoparticle properties depend strongly on their composition, size, shape, and surface chemistries.<sup>20</sup> In the present study, the toxicity and long-term biodistribution of

calcined 500 nm SiO<sub>2</sub> nanoshells and Fe-SiO<sub>2</sub> nanoshells, which have been shown to be biodegradable *in vitro*, are investigated when administered IV to mice at a clinically relevant dose. One attractive characteristic of hollow SiO<sub>2</sub> nanoshells is that due to their hollow core, more particles can be administered on a per mass basis. Approximately 70% of the nanoshell is hollow, therefore, on average an equivalent of 3× more particles can be administered on a mg/kg basis compared to solid nanoparticles of the same size. The particles are calcined, which offers long term stability for storage, and their nanoporous shell wall permits influx and efflux of drugs, gases, and other small molecules. These characteristics allow for this platform to potentially be used as an ultrasound contrast agent or for drug delivery.<sup>6–8</sup> Other platforms such as solid nanoparticles cannot carry gases due to their solid core, therefore solid nanoparticles do not have color Doppler ultrasound capabilities. In addition, 500 nm nanoshells have demonstrated to have good ultrasound imaging capabilities which are partly the reason why their toxicity is being evaluated in this study. By understanding the toxicology effects of new nanomaterial formulations, nanoparticles can be designed for decreased toxicity thereby creating more efficacious and safe therapeutic and diagnostic agents.

## Methods

### Materials

Tetramethyl orthosilicate (TMOS) was purchased from Sigma Aldrich Corp (St. Louis, Missouri). 500 nm amino-polystyrene beads were acquired from Polysciences Inc. (Warrington, Pennsylvania). Iron (III) ethoxide was acquired from Gelest Inc. (Morrisville, Pennsylvania). Potassium hydroxide was purchased from Fischer-Scientific (Pittsburg, Pennsylvania). 500 mM aqueous KOH was obtained by dissolving the KOH pellets in Milli-Q water. Nitric acid (HNO<sub>3</sub>) was provided by EMD (Billerica, Massachusetts) at 67%–70% purity and 1% HNO<sub>3</sub> was prepared by diluting the stock HNO<sub>3</sub> with MilliQ water. The multi-element standard solution for silicon calibration was provided by SPEX CertiPrep (Metuchen, New Jersey). The yttrium standard solution for internal calibration was purchased from Agilent Technologies (Santa Clara, California). Blood collection tubes coated in either heparin or EDTA were purchased from BD Biosciences (Franklin Lakes, New Jersey).

Six week old female Swiss Webster mice were provided by Charles River Laboratories, weighing between 20 and 25 g each. Mice were fed a commercial pelleted diet (Harlan Tekland) and kept at 22 °C in UCSD approved animal housing with a 12 h light/dark cycle. All animal care and procedures were approved by the UCSD Institutional Animal Care and Use Committee. All animals in these studies were treated with humane care.

### Nanoshell synthesis

Fe-SiO<sub>2</sub> and pure SiO<sub>2</sub> nanoshells were synthesized as previously reported.<sup>6,7</sup> Fe-SiO<sub>2</sub> nanoshells were synthesized by mixing of 2.7 µl of TMOS, 10 µl of iron ethoxide (20 mg/ml in ethanol), and 50 µl of amino-polystyrene templates in 1 ml of

absolute ethanol for 5 h on a vortex mixer at 3000 RPM. After mixing, the particles are centrifuged and washed three times in ethanol and left to dry overnight. Dry particles were then calcined for 18 h at 550 °C. Pure SiO<sub>2</sub> particles were synthesized by mixing 3 µl of TMOS and 50 µl of polystyrene templates in 1 ml of absolute ethanol for 5 h. After mixing, the particles were centrifuged and washed three times in ethanol and left to dry overnight. The dry particles were subsequently calcined for 18 h at 550 °C. Particle synthesis and quality were confirmed by scanning electron microscopy (SEM) and transmission electron microscopy (TEM). The diameter and shell thickness of nanoshells were quantified by measuring the diameter and length of the shell thickness taken from high resolution TEM images and analyzed using ImageJ. The percentage of hollow space occupied by the nanoshells was determined by calculating the volume of the hollow nanoshell using the outer diameter and subtracting the volume of the inner diameter of the nanoshell. SEM images were acquired using an FEI/Phillips XL30 FEG ESEM with an accelerating voltage of 10 kV. Energy dispersive X-ray spectroscopy (EDX) was performed on the same Oxford EDX attachment and analyzed with INCA software. TEM images were acquired using a JEOL 1200 EX II TEM.

#### *Single dose toxicity*

A single dose toxicity study was performed over the course of 10 weeks in healthy female Swiss white mice. Four groups were compared (n = 10) to determine if the nanoshells had any measureable toxicity. Group 1 received a 100 µl injection of Fe-SiO<sub>2</sub> nanoshells at 4 mg/ml (approximately 20 mg/kg), group 2 received 100 µl of SiO<sub>2</sub> nanoshells at 4 mg/ml, group 3 received 100 µl of SiO<sub>2</sub> nanoshells at 2 mg/ml (approximately 10 mg/kg) which is the particle number/ml equivalent of group 1 (Fe-SiO<sub>2</sub> at 4 mg/ml), and group 4 was a control group which received no particles. All injections were performed IV *via* the tail vein. 100 µl of blood was drawn with a submandibular lancet from each mouse weekly for the first four weeks and then biweekly for the following six weeks. From each group, 5 mice had their blood allocated into Vacutainer tubes containing EDTA for Complete Blood Count (CBC) analysis and the other 5 mice had their blood allocated into Vacutainer tubes containing heparin for serum chemistry analysis. CBC and Serum Chemistry analyses were performed by UCSD Animal Care Program Diagnostic Laboratory and STAT Labs. After 10 weeks, the animals were sacrificed. Three animals from each group were used for long-term biodistribution studies, and the remaining animals were used for pathological investigation after sectioning and H&E staining.

#### *Inductively coupled plasma optical emission spectroscopy (ICP-OES analysis)*

ICP-OES was used to detect nanoshells retained in mouse organs. One mouse was injected with 100 µl of a 4 mg/mL aqueous nanoshell solution. Control mice were sacrificed 24 h after the mice received the nanoshell injection, and the organs were collected. To analyze the organs for silicon content, the organs were incubated in 7 ml of aqueous 500 mM KOH and

bath sonicated for 48 h. 0.5 ml of each digested sample was drawn out and acidified using 2.5 ml of 1% HNO<sub>3</sub>. The samples were centrifuged for 15 min at 3000 rpm, and 0.5 ml of a 300 ppb yttrium standard solution was added to each 2.5 ml aliquot of a supernatant sample. The samples were finally briefly centrifuged immediately before ICP-OES analysis as described in a previous study.<sup>26</sup>

#### *Histological analysis*

Tissue samples were fixed in 10% formalin and submitted to the UCSD histology core facility for paraffin block processing, sectioning and Hematoxylin and Eosin (H&E) staining. The slides were imaged using a Nikon Eclipse E600 microscope. The slides were randomized and analyzed by the Chief of Pathology and Laboratory Medicine at the VA Medical Center, La Jolla. Focal inflammation was quantified by counting the number of inflammatory foci per organ for each group.

#### *Statistical analysis*

Serum chemistry and hematology markers were compared by using multiple unpaired two-tailed *t* tests to determine statistical significance (alpha = 0.05). Mean values were calculated for each time point in order to perform multiple *t* tests as described by J. N. Matthews, et al.<sup>27</sup> Statistical analysis was performed by using GraphPad Prism software version 6. A total number of 5 mice per group were used for the study.

## **Results**

#### *Characterization of nanoshells*

The SiO<sub>2</sub> and Fe-SiO<sub>2</sub> nanoshells were hollow and spherical in shape with an average diameter of 497 nm ± 13 and 455 nm ± 14, respectively, as shown by SEM and TEM in Figure 1. The images show that the SiO<sub>2</sub> and Fe-SiO<sub>2</sub> nanoshells are fairly uniform in size with no visible holes, cracks, or other deformations. The diameters and shell thicknesses of nanoshells were determined by using TEM images. The incorporation of iron does not greatly affect the shell thickness or morphology compared to pure SiO<sub>2</sub> nanoshells; the shell thickness for Fe-SiO<sub>2</sub> was 27 nm ± 4 and 33 nm ± 5 for SiO<sub>2</sub> nanoshells. EDX showed that Fe-SiO<sub>2</sub> nanoshells have an average 5 mol % of iron doped into the nanoshell matrix. The incorporation of iron makes the nanoshells biodegradable in human serum, and attractive for biomedical applications.<sup>28</sup> Serum transferrin has been shown to bind to the iron-doped nanoshells, which may induce degradation and dissolution of any residual nanoshells that are not excreted from the body.<sup>29</sup> In addition, 500 nm Fe-SiO<sub>2</sub> nanoshells may be filled with gases giving them ultrasound capabilities as shown in Figure 2.

#### *Single dose acute toxicity*

The 500 nm nanoshells evaluated in this study have been developed for use as contrast agents when filled with perfluoropentane gas or as ablative agents when combined with high intensity focused ultrasound (HIFU).<sup>2,6,30</sup> It is important to thoroughly evaluate the toxicity of new compounds



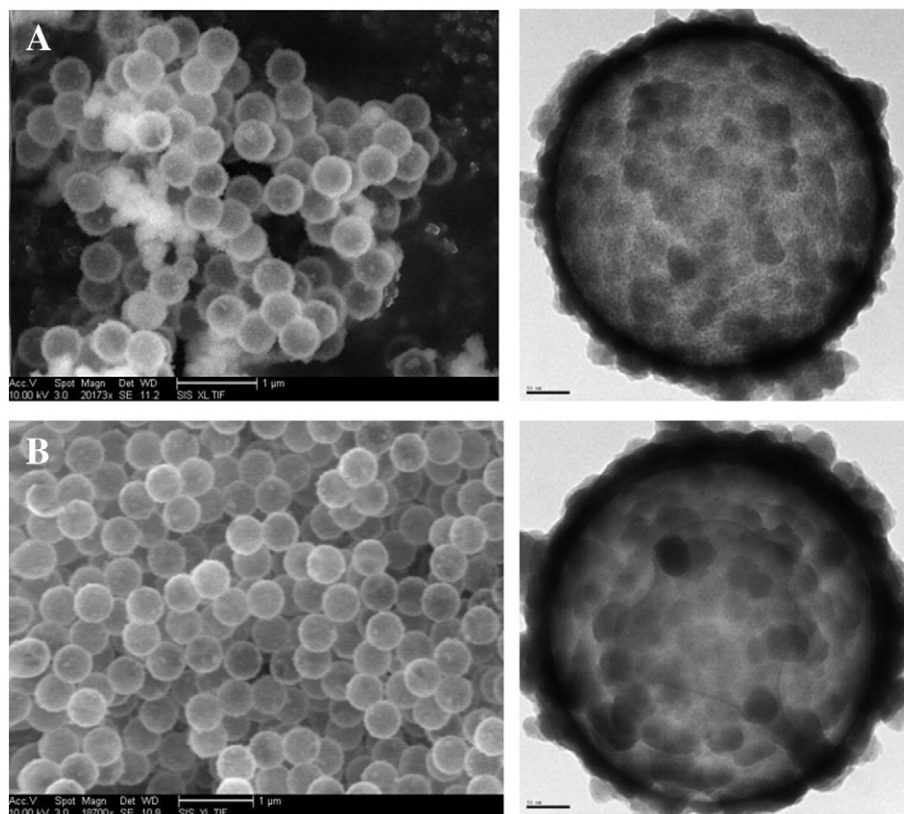


Figure 1. SEM and TEM images of 500 nm (A) Fe-SiO<sub>2</sub> and (B) SiO<sub>2</sub> nanoshells.

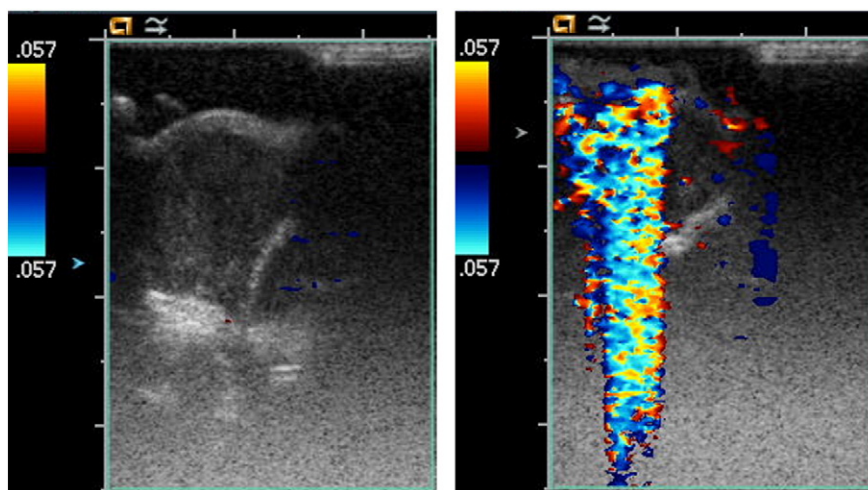


Figure 2. 500 nm SiO<sub>2</sub> and Fe-SiO<sub>2</sub> nanoshells have ultrasound imaging capabilities under color Doppler and CPS mode.

before the translation to clinical trials. Therefore, the acute toxicity of SiO<sub>2</sub> and Fe-SiO<sub>2</sub> nanoshells was assessed in order to evaluate their safety *in vivo*. Mice received an IV injection of 400 μg of SiO<sub>2</sub> (20 mg/kg), 400 μg of Fe-SiO<sub>2</sub> (20 mg/kg), 200 μg of SiO<sub>2</sub> (10 mg/kg), or Phosphate Buffered Saline (PBS). 10 mg/kg was assessed for SiO<sub>2</sub> because it is the equivalent of the Fe-SiO<sub>2</sub> by particle concentration. Blood was collected over the

course of 10 weeks and serum chemistry and hematology analysis were performed.

Nanoparticles have been shown to have different pharmacological actions when administered IV, depending on factors such as size, shape, charge, and composition. In particular, nanoparticles usually preferentially accumulate in the liver.<sup>3</sup> Therefore it is important to evaluate if nanoparticle administration affects

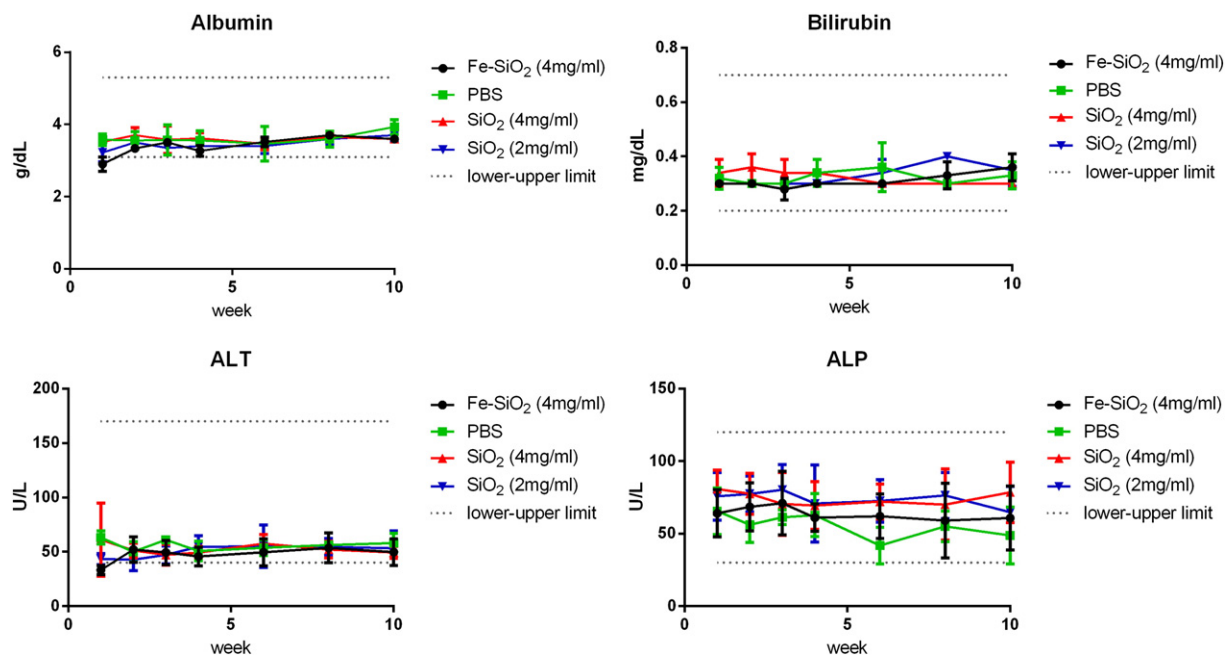


Figure 3. Serum chemistry analysis for hepatic function. Mice were injected with 100  $\mu$ l of Fe-SiO<sub>2</sub> nanoshells at 4 mg/ml (●), SiO<sub>2</sub> at 4 mg/ml (▲), SiO<sub>2</sub> nanoshells at 2 mg/ml (▼), or PBS (■). Albumin, bilirubin, alanine transaminase (ALT), and alkaline phosphatase (ALP) were measured in mice over the course of 10 weeks to evaluate hepatic function. Serum chemistry did not differ significantly between control and treated groups. Data are shown as average  $\pm$  SD, where  $n = 5$ .

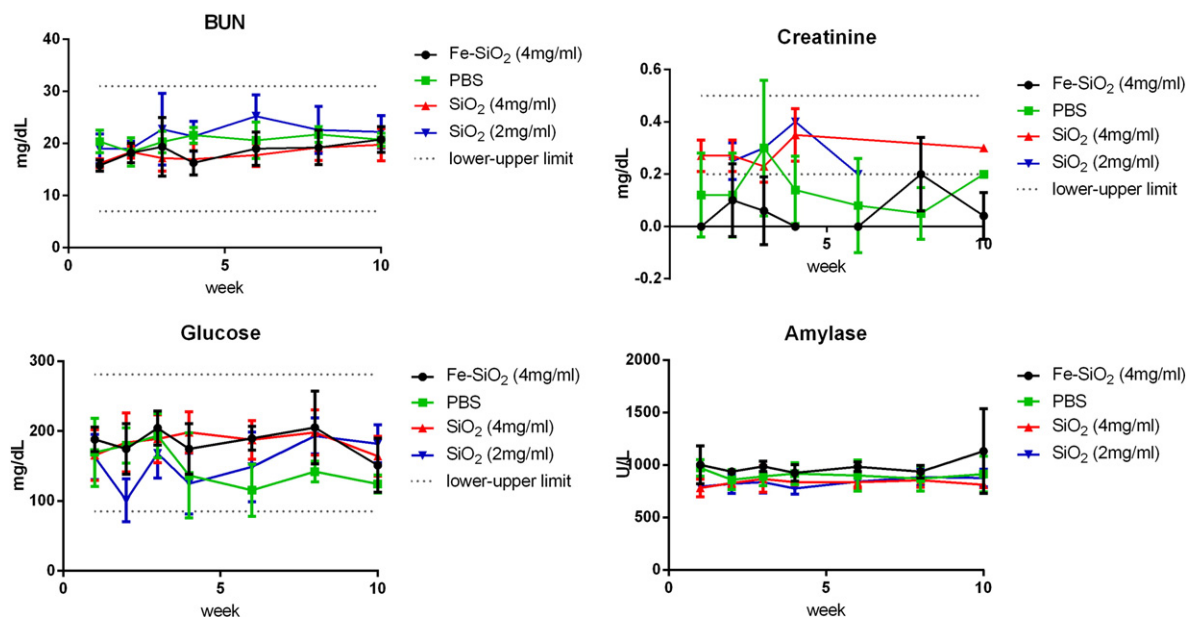


Figure 4. Serum chemistry analysis for renal and pancreatic function. Mice were injected with 100  $\mu$ l of Fe-SiO<sub>2</sub> nanoshells at 4 mg/ml (●), SiO<sub>2</sub> at 4 mg/ml (▲), SiO<sub>2</sub> nanoshells at 2 mg/ml (▼), or PBS (■). Blood urea nitrogen (BUN), creatinine, glucose and amylase were measured in mouse serum over the course of 10 weeks to evaluate general renal and pancreatic function. Serum chemistry did not differ significantly between control and treated groups. Data are shown as average  $\pm$  SD, where  $n = 5$ .

liver function. For serum chemical analysis, albumin, bilirubin, alanine transaminase (ALT), and alkaline phosphatase (ALP) were evaluated to assess hepatic function as shown in Figure 3. The serum chemistry levels for mice which received Fe-SiO<sub>2</sub> or

SiO<sub>2</sub> did not differ significantly from the control group. Multiple  $t$  tests were performed for statistical analysis and all groups showed no statistically significant difference between the control and nanoshell dosed groups ( $\alpha = 0.05$ ). These data indicate

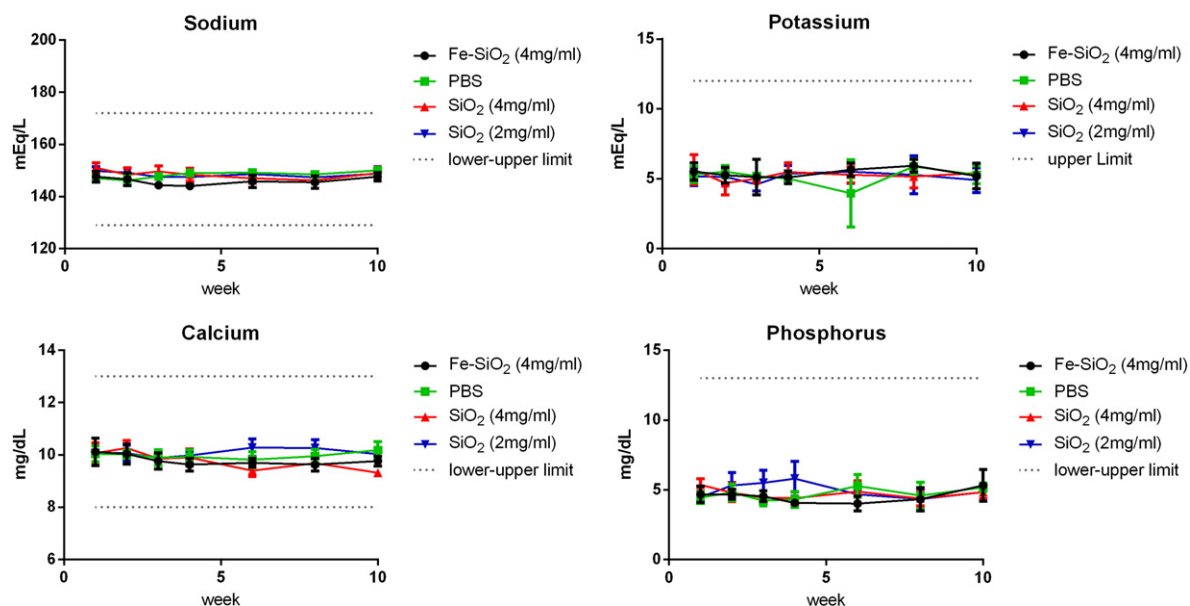


Figure 5. Serum chemistry analysis for electrolyte imbalance. Mice were injected with 100  $\mu$ l of Fe-SiO<sub>2</sub> nanoshells at 4 mg/ml (●), SiO<sub>2</sub> at 4 mg/ml (▲), SiO<sub>2</sub> nanoshells at 2 mg/ml (▼), or PBS (■). Sodium, potassium, calcium, and phosphorus were measured in mouse serum over the course of 10 weeks to evaluate electrolyte imbalance. Serum chemistry did not differ significantly between control and treated groups. Data are shown as average  $\pm$  SD, where  $n = 5$ .

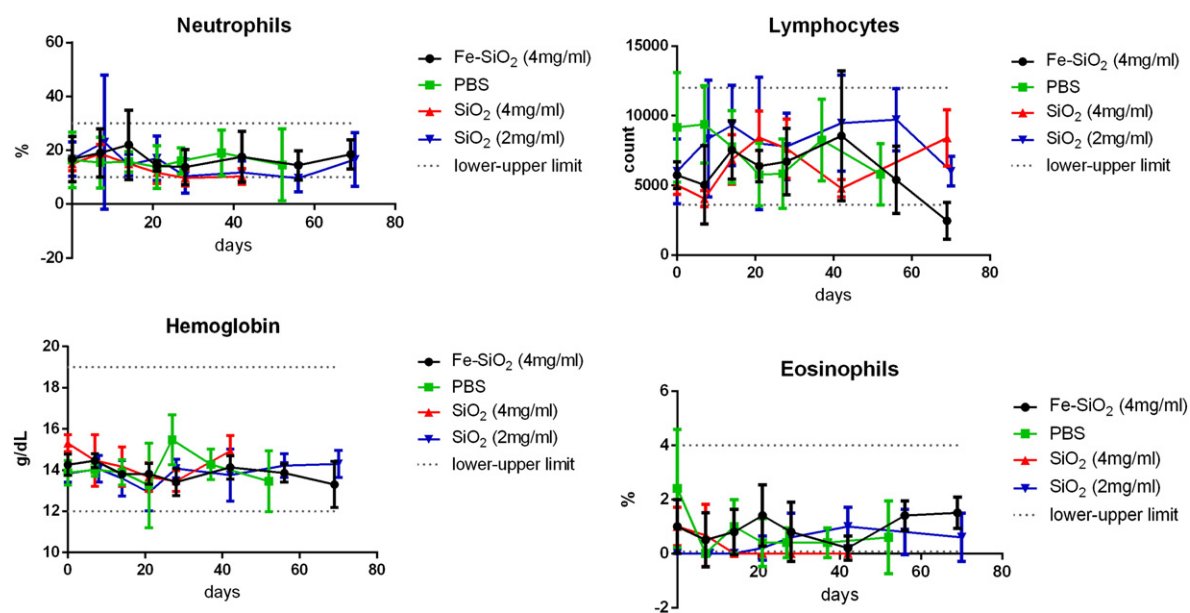


Figure 6. Mouse hematology. Mice were injected with 100  $\mu$ l of Fe-SiO<sub>2</sub> nanoshells at 4 mg/ml (●), SiO<sub>2</sub> at 4 mg/ml (▲), SiO<sub>2</sub> nanoshells at 2 mg/ml (▼), or PBS (■). Blood was collected over the course of 10 weeks and hematology tests were performed to assess blood, blood-forming organs, and blood diseases. No significant difference was observed between Fe-SiO<sub>2</sub> nanoshells, SiO<sub>2</sub> nanoshells, and PBS control. Data are shown as average  $\pm$  SD, where  $n = 5$ .

that a systemic dose of 20 mg/kg (4 mg/ml) of SiO<sub>2</sub> or Fe-SiO<sub>2</sub> nanoshells show no acute hepatic toxicity over the course of 10 weeks.

Nanoparticles have been shown capable of being cleared through the renal system.<sup>4</sup> Therefore blood urea nitrogen (BUN) and creatinine were measured to determine if IV administration of 500 nm SiO<sub>2</sub> and Fe-SiO<sub>2</sub> nanoshells alters renal function. Pancreatic function was also assessed by measuring amylase and

glucose as shown in Figure 4. The SiO<sub>2</sub> nanoshell group had a significantly higher serum creatinine levels compared to the control group ( $P = .003$  for 4 mg/ml  $P = .01$  for 2 mg/ml). However, for all groups the values were still within the normal range for serum creatinine values reported by Charles River for female Swiss Webster mice.

Serum analytes such as sodium (Na), potassium (K), calcium (Ca), and phosphorus (P) were measured in order to evaluate any



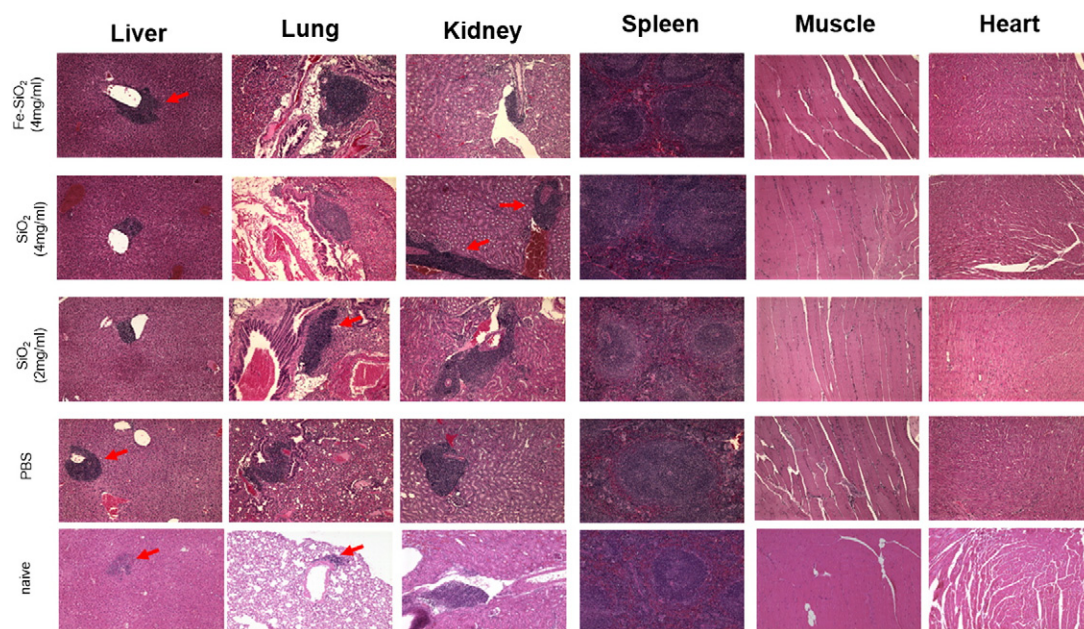


Figure 7. Histological analysis of Fe-SiO<sub>2</sub> and SiO<sub>2</sub> nanoshells. A single dose acute toxicity study was performed over the course of 10 weeks in healthy female Swiss white mice. Five groups were compared to determine if the nanoshells had any measureable toxicity; (A) Fe-SiO<sub>2</sub> (400 μg), (B) SiO<sub>2</sub> (400 μg), (C) SiO<sub>2</sub> (200 μg), (D) PBS and (E) naive group. Images are shown at 100×. Mild focal inflammation is observed in the liver, lung and kidney for all groups. Arrows are pointing to inflammation foci.

electrolyte imbalances of mice post injection as shown in Figure 5. There were significantly higher serum Na levels for mice that received Fe-SiO<sub>2</sub> when compared to the control group ( $P = .002$ ). Nevertheless, when compared to Na values reported by Charles River, the Na values measured in this study fell within the normal range of the 95% confidence interval. Overall, the general health of mice administered with Fe-SiO<sub>2</sub> and SiO<sub>2</sub> nanoshells IV was unaffected by the particles.

Amorphous SiO<sub>2</sub> particles have been shown to cause hemolysis of red blood cells which raises safety concerns about their use in the clinic.<sup>15,16</sup> The interaction of SiO<sub>2</sub> nanoparticles and blood components impacts cellular toxicity and hemolytic activity, which depend on different nanoshell formulations such as composition, size, and charge. Therefore, hematology analysis of 500 nm Fe-SiO<sub>2</sub> and SiO<sub>2</sub> nanoshells was performed in order to assess blood chemistry, blood-forming organs, and blood diseases. Neutrophils, lymphocytes, hemoglobin (Hb), and eosinophils were measured to assess hematological abnormalities after nanoshell administration over the course of ten weeks and as a potential indicator of an immune or inflammatory reaction, as shown in Figure 6. Other analytes such as monocytes, red blood cells (RBCs), nucleated RBCs/100 WBCs, mean corpuscular volume (MCV), mean corpuscular hemoglobin concentration (MCHC), and mean platelet volume (MPV) were also measured (see Figure S1). There was no significant difference observed between Fe-SiO<sub>2</sub> nanoshells, SiO<sub>2</sub> nanoshells at 2 mg/ml or 4 mg/ml, and the PBS vehicle group for any of the analytes. In addition, all measured values fell within the 95% CI values reported by Charles River. These findings are a good indication that SiO<sub>2</sub> and Fe-SiO<sub>2</sub> nanoshells are generally safe when administered systemically at

the indicated doses. It is likely that the physical characteristics of the nanoshells including their hollow core, surface composition, and size contributed to their low toxicity.

Hematoxylin and eosin (H&E) histological analysis was performed on liver, lung, kidney, spleen, muscle, and heart tissue samples 10 weeks after administration of Fe-SiO<sub>2</sub> or SiO<sub>2</sub> nanoshells to check for inflammation or any abnormalities, as shown in Figure 7. The pathology revealed some mild chronic inflammation in the liver, lung, and kidney in all groups as evidenced by focal lymphocytic infiltrates. Representative sections show lymphocytic infiltrate in the perisinusoidal distribution in the liver, peri-bronchial in the lung, and peri-vascular in the kidney. Histological analysis was also performed on the brain and showed no pathological changes when compared to the PBS control (see Figure S2). The number of mice with focal inflammation in each group was not significantly different in mice treated with nanoshells when compared to mice injected with PBS as summarized in Table 1.

In addition, the organs of naive mice which have no isoflurane anesthesia exposure or blood drawn were evaluated. Mild focal inflammation was observed in the lung and kidney, and acute inflammation was observed in the liver which shows that mild inflammation is typical in naive Swiss mice as shown in Figure 7, E. Similarly, Plummer et al.<sup>31</sup> showed that the control group as well as rats exposed to inhaled isoflurane anesthesia for a prolonged period of time showed hepatic focal inflammation suggesting that mild focal inflammation is often observed in healthy laboratory rodents. It is possible that repeat bleeding and isoflurane anesthesia are probable factors contributing to increased focal inflammation observed in our experimental and PBS control mice groups.<sup>32</sup>

Table 1  
Inflammation in major mouse organs.

	Lung	Kidney	Spleen	Muscle	Heart	Brain
Fe-SiO <sub>2</sub> (4 mg/ml)	71%	86%	0%	0%	0%	0%
SiO <sub>2</sub> (4 mg/ml)	60%	100%	0%	0%	0%	0%
SiO <sub>2</sub> (2 mg/ml)	43%	71%	86%	0%	0%	0%
PBS	71%	57%	71%	0%	0%	0%

Pathological evaluation of mouse liver, lung, kidney, spleen, muscle, heart, and brain showed mild inflammation in the liver, lung, and kidney of all groups. The percentage of mice which showed at least one focal point of inflammation in each organ is summarized per organ (n = 5 per group). Multiple *t* test analysis showed no statistical significance when compared to the control group.

No multinucleated cells were observed in the spleen. No abnormalities were noted for any of the H&E sections and no apparent differences were observed between mice treated with Fe-SiO<sub>2</sub> or SiO<sub>2</sub> nanoshells and the PBS group. The number of inflammatory foci was quantified to evaluate the degree of focal inflammation per group as shown in Figure 8. There were no significant differences between groups treated with Fe-SiO<sub>2</sub> or SiO<sub>2</sub> nanoshells and the control group. These results showed that there was no significant damage to major organs (liver, lungs, heart, kidney, and spleen) when compared to control mice. This indicates that Fe-SiO<sub>2</sub> and SiO<sub>2</sub> nanoshells can potentially be safely used in the clinic by IV dosing at the given doses.

The biodistribution of Fe-SiO<sub>2</sub> and SiO<sub>2</sub> nanoshells was performed 24 h or 10 weeks after systemic administration, and ICP-OES was used to measure the amount of elemental Si in each organ, as shown in Figure 9.

For SiO<sub>2</sub> nanoshells, 42% of total injected nanoshells accumulated in the liver, which is consistent with previous studies.<sup>7</sup> It is important to note that nearly 57% of the total injected dose was not detected in any organs or the blood 24 h after administration; this may be due to excretion. After 10 weeks post administration, only 2% of nanoshells were detected in the liver. Similarly, the biodistribution of Fe-SiO<sub>2</sub> was studied 24 h and 10 weeks post-injection. Interestingly, when SiO<sub>2</sub> nanoshells were doped with iron, only 5% of the total injected dose was present in the liver, while 8% was detected in the lungs. Nearly 88% of the total injected dose was undetectable in the organs or the blood after only 24 h. After 10 weeks post administration, only 4% of nanoshells were detected in organs, mostly in the liver.

In a previous study, whole body scintigraphy in a mouse showed that after IV administration, a large portion of Fe-SiO<sub>2</sub> and SiO<sub>2</sub> nanoshells localized in the liver when monitored immediately post injection and at 1 h, 24 h, and 72 h.<sup>7</sup> After 72 h, organ gamma counting showed a substantial amount of signal in the liver, and some in the kidney and spleen, but very little signal was detected elsewhere. The results in the present study show that the nanoshells are retained mostly by the liver and suggest that incorporation of iron can alter the biodistribution of SiO<sub>2</sub> nanoshells. These findings show that fewer nanoshells were retained within 24 h when they were doped with iron. It is postulated that iron doping leads to transferrin interactions in the body which may lead to faster biodegradation as seen in previous studies.<sup>28</sup>

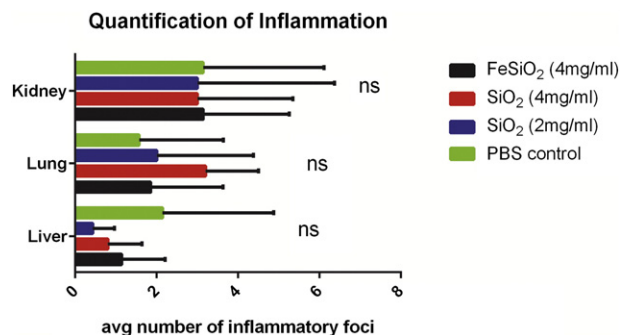


Figure 8. Quantification of focal inflammation in liver, lung, and kidney. Focal inflammation was quantified by counting the total number of focal inflammation foci for each mouse and computing the average per group. Multiple *t* tests showed no statistical significance (ns) when compared to the control group.

## Discussion

The kidney is capable of removing molecules from the blood by filtering particles through the glomerular capillary wall, also known as glomerular filtration. Renal filtration depends on surface charge and size, where molecules with a hydrodynamic diameter greater than 8 nm are typically not capable of glomerular filtration and therefore are not excreted *via* the renal system<sup>33,34</sup>; however, some studies have suggested that particles larger than 8 nm can be excreted through the urine.<sup>4</sup> Nevertheless, it is highly unlikely that a large number or intact 500 nm SiO<sub>2</sub> nanoshells are being excreted in the urine unless the particles were first broken down to smaller components before renal excretion.

The liver catabolizes particles in the blood through phagocytosis followed by biliary excretion.<sup>34</sup> Phagocytic Kupffer cells, specialized macrophages located in the liver, are highly effective at recognizing and removing unwanted substances from the blood, including nano- and microparticles. Kupffer cells selectively phagocytose opsonized particulates which have been coated with complement proteins for recognition.<sup>35,36</sup> Particles are subsequently metabolized and excreted as bile *via* the biliary system. Passage through the liver can make metabolites smaller and more polar which can result in reabsorption in the blood leading to excretion *via* the renal system; however, renal clearance is observed at lower rates. In the present study, it is most likely that the particles are being cleared *via* the hepatic system. It is hypothesized that iron incorporation can alter the uptake, metabolism, and clearance of the nanoshells. It is probable that the interaction of serum proteins is different for Fe-SiO<sub>2</sub> and SiO<sub>2</sub> nanoshells, which may result in a different extent of opsonization for each formulation. The altered surface protein coating of the Fe-SiO<sub>2</sub> nanoshells may change the extent of Kupffer cell phagocytosis and hepatic excretion.

The main site of transferrin synthesis is in the liver.<sup>37</sup> Transferrin is an iron transport protein that delivers Fe<sup>3+</sup> from the duodenum and macrophages to all tissues by circulating in the blood.<sup>38</sup> Human transferrin binds iron as Fe<sup>3+</sup> with a high affinity; therefore, the incorporation of Fe<sup>3+</sup> into the SiO<sub>2</sub> nanoshell structure likely facilitates the decomposition of



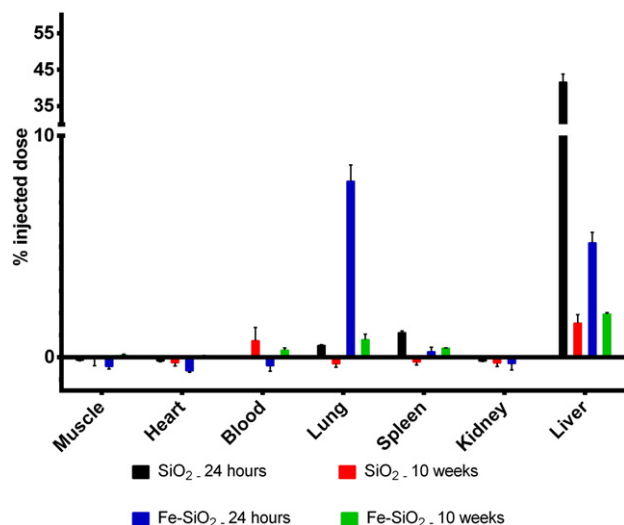


Figure 9. Biodistribution of SiO<sub>2</sub> after IV administration. 500 nm SiO<sub>2</sub> nanoshells and Fe-SiO<sub>2</sub> nanoshells were administered IV to mice. Mice were sacrificed and organs were collected 24 h or 10 weeks post-treatment. ICP-OES analysis was used to detect silica content in each organ. High accumulation of SiO<sub>2</sub> nanoshells was observed 24 h post administration, and clearance occurred after 10 weeks. Fe-SiO<sub>2</sub> nanoshells showed reduced uptake in the liver but some uptake in the lung after 24 h. Both SiO<sub>2</sub> and Fe-SiO<sub>2</sub> showed very low levels of detectable silica in organs 10 weeks after administration. Data are shown as average  $\pm$  SD.

Fe-SiO<sub>2</sub> nanoshells by degradation, which results in hepatic clearance. The biodegradation of Fe-SiO<sub>2</sub> in FBS and human serum was shown in previous studies,<sup>28</sup> consistent with the *in vivo* results shown in the present study. More recent studies show that Fe-SiO<sub>2</sub> nanoshells undergo binding/endocytosis in cells that overexpress the transferrin receptor and that their uptake can be blocked with addition of holotransferrin.<sup>29</sup> This suggests that the surface of the Fe-SiO<sub>2</sub> nanoshells may also be bound to transferrin *in vivo*. Not only are hepatocytes involved in iron metabolism, but the liver endothelium has been shown to be rich in the transferrin receptor, which enhances endocytosis of the Fe-SiO<sub>2</sub> nanoshells.<sup>39–41</sup> The liver endothelium has an increasingly recognized role in biliary excretion.<sup>42</sup>

A small percentage of Fe-SiO<sub>2</sub> nanoshells was observed in the lung, whereas only trace amounts of non-doped SiO<sub>2</sub> nanoshells were seen. Previous studies have shown that SiO<sub>2</sub> nanoparticles can cause an inflammatory response in the lung.<sup>33</sup> Kusaka et al showed that 30 nm SiO<sub>2</sub> nanoparticles administered intratracheally to mice caused more severe lung inflammation than did 3000 nm SiO<sub>2</sub> particles.<sup>43</sup> The present study shows that there was no additional long-term lung damage after 500 nm Fe-SiO<sub>2</sub> and SiO<sub>2</sub> nanoshells were administered IV when compared to the control group, which may be due to their larger size and/or the difference in route of administration. Several studies have been performed in order to assess the toxicity of SiO<sub>2</sub> nano- and microparticles<sup>11,25,44,45,46</sup> which showed that the SiO<sub>2</sub> particle biodistribution depends on several factors such as charge, size, and surface modification.

These nanoshells are expected to be used as contrast agents for cancer diagnosis or for ultrasound guidance during surgery.

In previous studies, the nanoshells have shown to be stationary markers *in vivo* and can be imaged intermittently over the course of 10 days in a tumor-bearing mouse model, and continuously for 45 min when administered intratumorally.<sup>30</sup> In the event that the nanoshells escape the tumor or are administered IV, this study has shown that the nanoshells show no apparent systemic toxicity and can be safely cleared from the body after a single dose. In addition, these nanoshells may also be used in combination with HIFU for ablative therapy.<sup>2</sup>

These results show that the nanoshells presented in this study are safe when administered systemically allowing exploitation of the hollow structure and calcined shells. Approximately 70% of the nanoshell is hollow, therefore, on average an equivalent of 3 $\times$  more particles can be administered on a mg/kg basis compared to solid nanoparticles of the same size. The particles are calcined, which offers long term stability for storage, and their nanoporous shell wall can permit influx and efflux of drugs, gases, and other small molecules. Although future pharmacokinetic studies including blood circulation and clearance should be performed, this study indicates that 500 nm nanoshells are safe when administered IV at the doses studied.

## Acknowledgment

The authors thank the Cancer Center Microscopy Core Facility at UCSD and the UCSD Histology and Immunohistochemistry core facility.

## Appendix A. Supplementary data

Supplementary data to this article can be found online at <http://dx.doi.org/10.1016/j.nano.2016.10.018>.

## References

1. Tan W, Wang K, He X, Zhao XJ, Drake T, Wang L, et al. Bionanotechnology based on silica nanoparticles. *Med Res Rev* 2004;24:621–38.
2. Liberman A, Wu Z, Barback CV, Viveros RD, Wang J, Ellies LG, et al. Hollow iron-silica nanoshells for enhanced high intensity focused ultrasound. *J Surg Res* 2014;190:391–8.
3. Liberman A, Mendez N, Troglor WC, Kummel AC. Synthesis and surface functionalization of silica nanoparticles for nanomedicine. *Surf Sci Rep* 2014;69:132–58.
4. Huang X, Li L, Liu T, Hao N, Liu H, Chen D, et al. The shape effect of mesoporous silica nanoparticles on biodistribution, clearance, and biocompatibility *in vivo*. *ACS Nano* 2011;5:5390–9.
5. Chen Y, Chen H, Shi J. *In vivo* bio-safety evaluations and diagnostic/therapeutic applications of chemically designed mesoporous silica nanoparticles. *Adv Mater* 2013;25:3144–76.
6. Liberman A, Martinez HP, Ta CN, Barback CV, Mattrey RF, Kono Y, et al. Hollow silica and silica-boron nano/microparticles for contrast-enhanced ultrasound to detect small tumors. *Biomaterials* 2012;33:5124–9.
7. Liberman A, Wu Z, Barback CV, Viveros R, Blair SL, Ellies LG, et al. Color Doppler ultrasound and gamma imaging of intratumorally injected 500 nm iron-silica nanoshells. *ACS Nano* 2013;7:6367–77.
8. Martinez HP, Kono Y, Blair SL, Sandoval S, Wang-Rodriguez J, Mattrey RF, et al. Hard shell gas-filled contrast enhancement particles

- for colour Doppler ultrasound imaging of tumors. *MedChemComm* 2010;**1**:266–70.
9. Park J-H, Gu L, von Maltzahn G, Ruoslahti E, Bhatia SN, Sailor MJ. Biodegradable luminescent porous silicon nanoparticles for in vivo applications. *Nat Mater* 2009;**8**:331–6.
  10. Wu P, He X, Wang K, Tan W, Ma D, Yang W, et al. Imaging breast cancer cells and tissues using peptide-labeled fluorescent silica nanoparticles. *J Nanosci Nanotechnol* 2008;**8**:2483–7.
  11. Decuzzi P, Godin B, Tanaka T, Lee SY, Chiappini C, Liu X, et al. Size and shape effects in the biodistribution of intravascularly injected particles. *J Control Release* 2010;**141**:320–7.
  12. Ji X, Shao R, Elliott AM, Stafford RJ, Esparza-Coss E, Bankson JA, et al. Bifunctional gold nanoshells with a superparamagnetic iron oxide-silica core suitable for both MR imaging and photothermal therapy. *J Phys Chem C* 2007;**111**:6245–51.
  13. Erogbogbo F, Yong K-T, Hu R, Law W-C, Ding H, Chang C-W, et al. Biocompatible magnetofluorescent probes: luminescent silicon quantum dots coupled with superparamagnetic iron (III) oxide. *ACS Nano* 2010;**4**:5131–8.
  14. Thorek DL, Chen AK, Czupryna J, Tsourkas A. Superparamagnetic iron oxide nanoparticle probes for molecular imaging. *Ann Biomed Eng* 2006;**34**:23–38.
  15. Slowing II, Wu C-W, Vivero-Escoto JL, Lin VSY. Mesoporous silica nanoparticles for reducing hemolytic activity towards mammalian red blood cells. *Small* 2009;**5**:57–62.
  16. Nash T, Allison AC, Harington JS. Physico-chemical properties of silica in relation to its toxicity. *Nature* 1966;**210**:259–61.
  17. Lu X, Tian Y, Zhao Q, Jin T, Xiao S, Fan X. Integrated metabolomics analysis of the size-response relationship of silica nanoparticles-induced toxicity in mice. *Nanotechnology* 2011;**22**:055101.
  18. Cho M, Cho W-S, Choi M, Kim SJ, Han BS, Kim SH, et al. The impact of size on tissue distribution and elimination by single intravenous injection of silica nanoparticles. *Toxicol Lett* 2009;**189**:177–83.
  19. Liu T, Li L, Teng X, Huang X, Liu H, Chen D, et al. Single and repeated dose toxicity of mesoporous hollow silica nanoparticles in intravenously exposed mice. *Biomaterials* 2011;**32**:1657–68.
  20. Chen Y, Chen H, Shi J. In vivo bio-safety evaluations and diagnostic/therapeutic applications of chemically designed mesoporous silica nanoparticles. *Adv Mater* 2013;**25**:3144–76.
  21. Zhang H, Dunphy DR, Jiang X, Meng H, Sun B, Tarn D, et al. Processing pathway dependence of amorphous silica nanoparticle toxicity: colloidal vs pyrolytic. *J Am Chem Soc* 2012;**134**:15790–804.
  22. Yu T, Greish K, McGill LD, Ray A, Ghandehari H. Influence of geometry, porosity, and surface characteristics of silica nanoparticles on acute toxicity: their vasculature effect and tolerance threshold. *ACS Nano* 2012;**6**:2289–301.
  23. Nishimori H, Kondoh M, Isoda K, Tsunoda S-I, Tsutsumi Y, Yagi K. Silica nanoparticles as hepatotoxicants. *Eur J Pharm Biopharm* 2009;**72**:496–501.
  24. He Q, Zhang Z, Gao F, Li Y, Shi J. In vivo biodistribution and urinary excretion of mesoporous silica nanoparticles: effects of particle size and PEGylation. *Small* 2011;**7**:271–80.
  25. Souris JS, Lee C-H, Cheng S-H, Chen C-T, Yang C-S, Ho J-aA, et al. Surface charge-mediated rapid hepatobiliary excretion of mesoporous silica nanoparticles. *Biomaterials* 2010;**31**:5564–74.
  26. Viveros RD, Liberman A, Trogler WC, Kummel AC. Alkaline and ultrasonic dissolution of biological materials for trace silicon determination. *J Vac Sci Technol B Nanotechnol Microelectron* 2015;**33**:031803.
  27. Matthews JN, Altman DG, Campbell MJ, Royston P. Analysis of serial measurements in medical research. *Br Med J* 1990;**300**:230–5.
  28. Pohaku Mitchell KK, Liberman A, Kummel AC, Trogler WC. Iron(III)-doped, silica nanoshells: a biodegradable form of silica. *J Am Chem Soc* 2012;**134**:13997–4003.
  29. Mitchell KP, Sandoval S, Cortes-Mateos MJ, Alfaro JG, Kummel AC, Trogler WC. Self-assembled targeting of cancer cells by iron (iii)-doped, silica nanoparticles. *J Mater Chem B Mater Biol Med* 2014;**2**:8017–25.
  30. Liberman A, Wang J, Lu N, Viveros RD, Allen CA, Mattrey RF, et al. Mechanically tunable hollow silica ultrathin nanoshells for ultrasound contrast agents. *Adv Funct Mater* 2015;**25**:4049–57.
  31. Plummer J, Hall PM, Jenner M, Ilsley A, Cousins M. Effects of chronic inhalation of halothane, enflurane or isoflurane in rats. *Br J Anaesth* 1986;**58**:517–23.
  32. Liu H, Xiao X, Sun C, Sun D, Li Y, Yang M. Systemic inflammation and multiple organ injury in traumatic hemorrhagic shock. *Front Biosci* 2015;**20**:927–33.
  33. Deen WM, Lazzara MJ, Myers BD. Structural determinants of glomerular permeability. *Am J Physiol Renal Physiol* 2001;**281**:F579–96.
  34. Longmire M, Choyke PL, Kobayashi H. Clearance properties of nano-sized particles and molecules as imaging agents: considerations and caveats. *Nanomedicine* 2008;**3**:703–17.
  35. Jaeschke H, Farhood A, Bautista AP, Spolarics Z, Spitzer JJ. Complement activates Kupffer cells and neutrophils during reperfusion after hepatic ischemia. *Am J Physiol* 1993;**264**:G801–9.
  36. Owens Ii DE, Peppas NA. Opsonization, biodistribution, and pharmacokinetics of polymeric nanoparticles. *Int J Pharm* 2006;**307**:93–102.
  37. Brissot P, Wright TL, Ma WL, Weisiger RA. Efficient clearance of non-transferrin-bound iron by rat liver. Implications for hepatic iron loading in iron overload states. *J Clin Invest* 1985;**76**:1463–70.
  38. Crichton RR, Charleaux-Wauters M. Iron transport and storage. *Eur J Biochem* 1987;**164**:485–506.
  39. Brieland JK, Clarke SJ, Karmiol S, Phan SH, Fantone JC. Transferrin: a potential source of iron for oxygen free radical-mediated endothelial cell injury. *Arch Biochem Biophys* 1992;**294**:265–70.
  40. Morgan EH, Baker E. Iron uptake and metabolism by hepatocytes. *Fed Proc* 1986;**45**:2810–6.
  41. Soda R, Tavassoli M. Liver endothelium and not hepatocytes or Kupffer cells have transferrin receptors. *Blood* 1984;**63**:270–6.
  42. Smedsrød B, Pertoft H, Gustafson S, Laurent TC. Scavenger functions of the liver endothelial cell. *Biochem J* 1990;**266**:313–27.
  43. Kusaka T, Nakayama M, Nakamura K, Ishimiya M, Furusawa E, Ogasawara K. Effect of silica particle size on macrophage inflammatory responses. *PLoS One* 2014;**9**.
  44. Yu T, Hubbard D, Ray A, Ghandehari H. In vivo biodistribution and pharmacokinetics of silica nanoparticles as a function of geometry, porosity and surface characteristics. *J Control Release* 2012;**163**:46–54.
  45. He X, Nie H, Wang K, Tan W, Wu X, Zhang P. In vivo study of biodistribution and urinary excretion of surface-modified silica nanoparticles. *Anal Chem* 2008;**80**:9597–603.
  46. Kumar R, Roy I, Ohulchanskyy TY, Vathy LA, Bergey EJ, Sajjad M, et al. In vivo biodistribution and clearance studies using multimodal organically modified silica nanoparticles. *ACS Nano* 2010;**4**:699–708.